Chapter – 5

Synthesis of Lawsone Vanadium complex for catalytic oxidation of diphenylmethane

5.1 Introduction

The selective oxidation of aryl alkanes (especially sp^3 C-H oxidation) bonds is one of the most challenging and important transformations both in academia and industry [1,2]. This protocol is important in industry as it can reduce number of steps towards target molecule in total synthesis and reduces overall time and cost [3]. The oxidation of diphenylmethane to benzophenone is gathering much attention as a model C-H oxy functionalization reaction. As it is key intermediate for synthesis of API, chemical building blocks, photo initiator, perfumes and insecticide[4]. Direct oxidation process of diphenylbenzene to benzophenone involves various oxidants such as, metal oxides, peroxides and halides[5–7]. These processes also involves strong oxidizing agents $KMnO_4$ or CrO_3 which produces a large volume of toxic wastes and causes series of environmental issues [8].

For the oxidation of arylalkanes, numerous techniques employing homogeneous and/or heterogeneous catalysts using noble metals such as Au, Rh, Ru, Pd, and Ir have recently been published [9–13]. Catalyst involving non-noble metals such as Fe, Cu, Mn, and V have also been reported[14–17]. Despite these significant improvements, activity, atom economy, and catalyst preparation costs remain unsatisfactory. As a result, there is still a strong desire to investigate more effective catalyst systems for arylalkane oxidation under long-term reaction conditions. Due to the importance of the catalyst in this process, research is still ongoing to find suitable catalysts.

Recently, Stahn S. S. and co-workers have reported the cobalt (II)/N-hydroxypthalimide (NPHI) catalyst system for selective conversion of benzylic methylene group. The reaction proceeds under practical reaction condition of 12 h at 90-100 °C in ethyl acetate or butyl acetate and proceeds via free radical pathway [18]. Lie A et al. has developed photo catalyst for benzylic C-H oxidation [19]. Wang wei and group have reported recyclable new TEMPO derived sulfonic salt catalyst, and mineral acids ($NaNO_2$ and HCl) for selective oxidation of benzylic C-H bond of ethers and arylarenes. Some other catalytic systems like N-hetrocyclic carbenes, KBr-Oxones and DDQ-t-butyl-nitrite were also developed for oxidation reaction. [20–22]. However, it can been seen that all these catalyst works under special conditions or in presence of co-catalyst or phase transfer agents. This literature emphasizes that developing a mild, efficient and environment friendly method for benzylic C-H oxidation still requires efforts.

Herein, we have synthesized vanadium (IV) **complex 10** derived from naturally occurring lawsone. The synthesized vanadium **complex 10** was characterized by FTIR, Uv-Visible, ESI-MS, powder XRD and EPR spectroscopy. The geometry of complex was also optimized using DFT calculations. The synthesized vanadium **complex 10** was successfully applied as catalyst for selective oxidation of diphenylmethane to benzophenone under mild condition with 96% conversion and selectivity.

5.2 Result and Discussion

5.2.1 Synthesis of complex 10

The **complex 10** was synthesized in good yield from the reaction of **1** with vanadyl acetyl acetonate using ethanol as a solvent at 30°C. The ethanolic solution of vanadyl acetyl acetonate was added dropwise to the suspension of lawsone in ethanol as shown in **scheme 5.1**. As soon as the addition of vanadyl acetyl acetonate was completed, the clear dark brown solution was observed. The resulting mixture was stirred for at 30°C 12 hr and kept it overnight. The dark brown crystalline powder was obtained after concentration under vacuum. The complex was isolated by filtration and given washing with hot water followed by chilled ethanol. The formation of complex was confirmed by various spectroscopic and analytical techniques such as FT-IR, UV-Visible, EPR, and ESI-MS. The synthesized complex was stable in the solid state. The powder XRD further confirms the crystalline nature of **complex 10**.

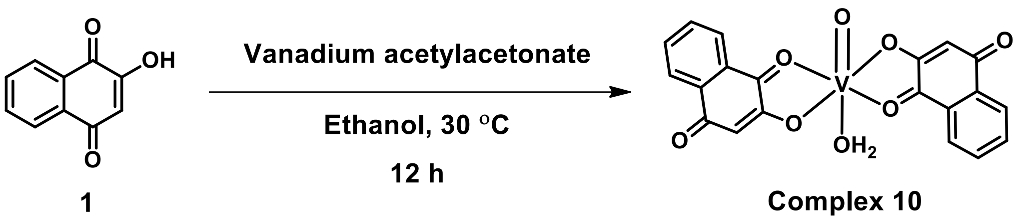

Scheme 5.1 Schematic for synthesis of complex 10

5.2.2 Spectral characterization

The FT-IR spectra showed a broad band near 3430 cm^{-1} corresponds to the stretching frequency of hydroxyl group for lawsone, while **complex 10** showed road band near 3389 cm^{-1} may be due to weakly coordinated water to vanadium metal **(figure 5.1).** The shift in carbonyl stretching frequency from 1678 cm^{-1} to 1650 cm^{-1} as compared to **1** (**figure 4.1)** confirms the participation of the carbonyl group in complex formation. Similarly, approx 20 cm^{-1} shift in C-O stretching frequency was observed in complex 10 as compared to **1.** Furthermore, the sharp band of V=O stretching frequency at 990 cm^{-1} confirm the formation of desired vanadium (IV) **complex 10** [23]**.**

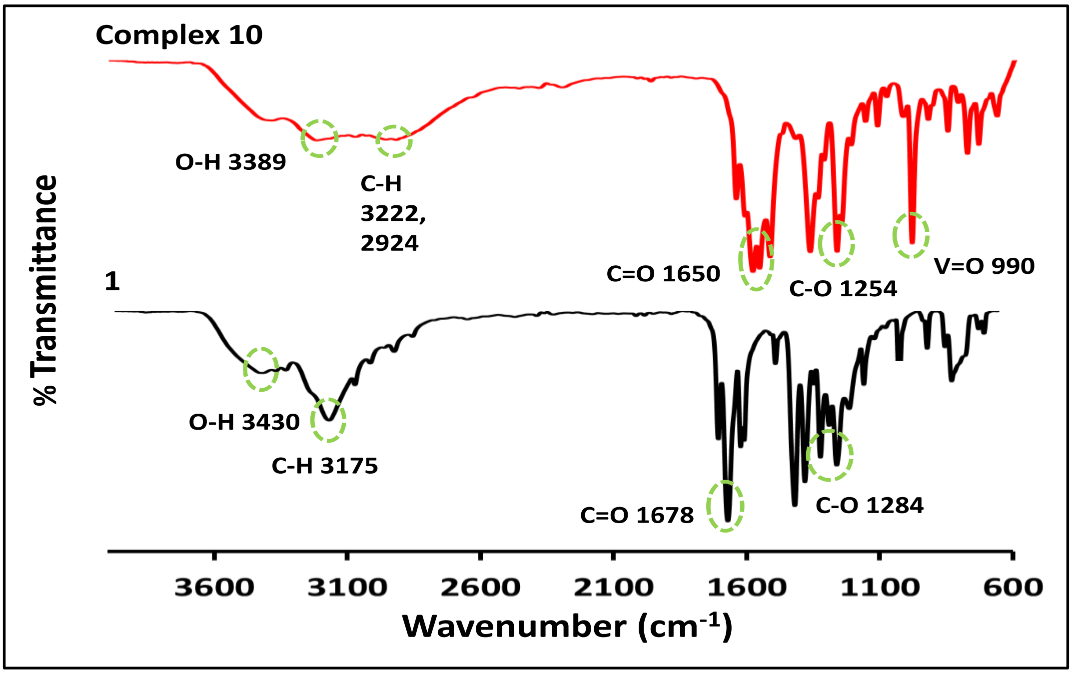

Figure 5.1 FT-IR spectra of complex 10 and 1

UV–Vis spectra of ligand **1** and **complex 10** were recorded in methanol as shown in **figure 5.2.** The shoulder like broad band was observed between 445 nm for the **1**. It can be attributed to n- $\pi*$ transition of the oxygen atom of lawsone quinoid ring. This band showed a red shift and was observed at 469 nm for **complex 10**. It can be attributed to metal-to-ligand charge transfer (MLCT) of the naphthoquinone moiety to the metal ion.

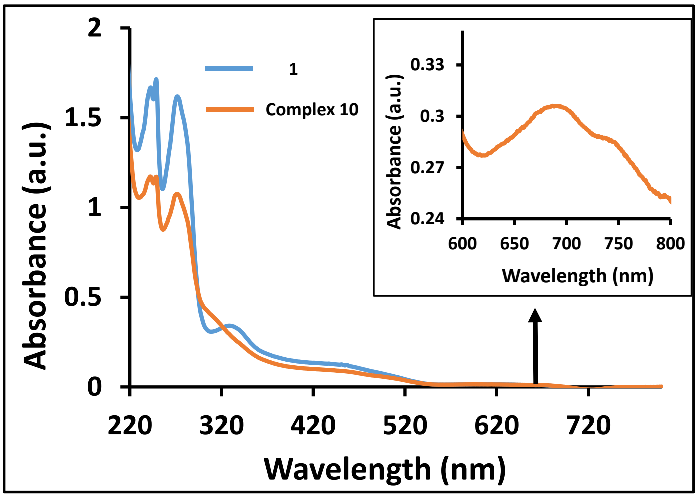

Figure 5.2 UV-visible spectra of 1, and complex 10

The low intensity d-d absorbance band at 690 nm for **complex 10** confirms the presence of VO^{2+} ion **(inset figure 5.2).** These bands ($E_g \rightarrow T_{2g}$) are typical for distorted octahedral VO^{2+} complex [24]**.** The π-π* band was also observed for all ligands 235-250 nm**,** which remains unaltered after complexation.

The molar conductance of **1** and **complex 10** were recorded in methanol (1.0×10^{-3} M). It revealed that both are non-electrolytic in nature. The molar conductance values were found to be 6.8 and 16.74 S cm^2 mol^{-1} for **1** and **complex 10** respectively.

The mass spectra of **complex 10** exhibited a peak at m/z = 431.1 corresponds to molecular ion peak $[C_{20}H_{12}O_8V]^+$ which confirms the formation of **complex 10 (figure 5.3).**

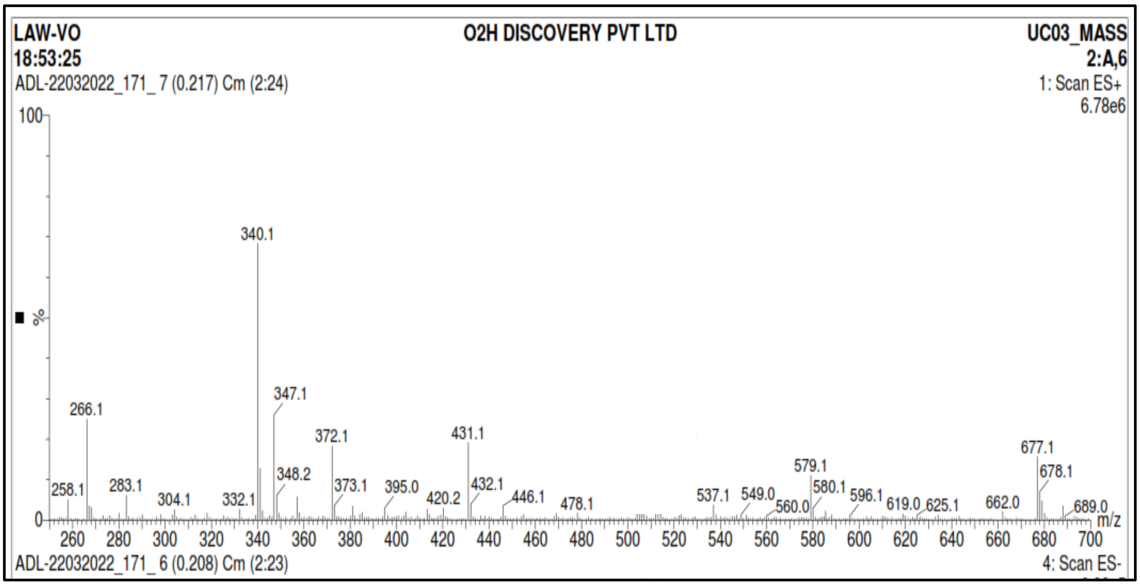

Figure 5.3 ESI-MS spectrum of complex 10

In order to ascertain the oxidation state of vanadium, X band EPR spectra of complexes were recorded at 100K temperature in DMSO **(figure 5.4).** The spectra exhibit an axially symmetrical hyperfine eight-line pattern that originates from d electron interaction with a nuclear spin I = 7/2. Thus spectra display well resolved ^{51}V hyperfine lines and signal parameters for the complexes are given in **table 5.1**.

Table 5.1 EPR parameters of complex 10

compound	$g_{\parallel}$	$g_{\perp}$	g_0	$A_{\parallel}(\times 10^{-4}\ cm^{-1})$	$A_{\perp}(\times 10^{-4}\ cm^{-1})$
Complex 10	2.009	1.9966	2.0048	175.958	73.397

The $g_{\parallel} >> g_{\perp}$ and $A_{\parallel} >> A_{\perp}$ relationships are characteristics of an axially compressed d_{xy} configuration. Thus, an oxidation state of +4 can be assigned to vanadium similar to other oxovanadium complexes reported earlier [25,26].

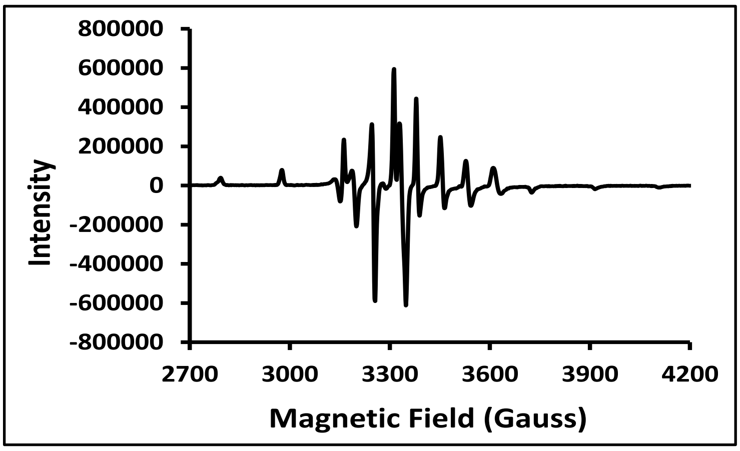

Figure 5.4 EPR spectra of complex 10

The powder X-ray diffraction (XRD) pattern of vanadium (IV) **complex 10** overlayed with ligand **L** shown in **figure 5**. The diffraction pattern was recorded from 2θ = 10 to 60°. The ligand L showed the peak at 2θ = 11.47°, 12.48°, 14.76°, 16.38°, 17.74°, 23.15°, 27.11°, 28.68°, 35.26°, 37.79°, 43.36° and 43.56°. while, the **complex 10** displayed peaks at 2θ = 10.71°, 12.6°, 13.90°, 14.76°, 15.77°, 16.28° ,17.34°, 20.93°, 22.25°, 23.77°, 24.39°, 24.83°, 25.34°, 26.50°, 28.02°, 29.94°, 31.61°, 32.48°, 35.06°, 45.74°, and 47.21°.

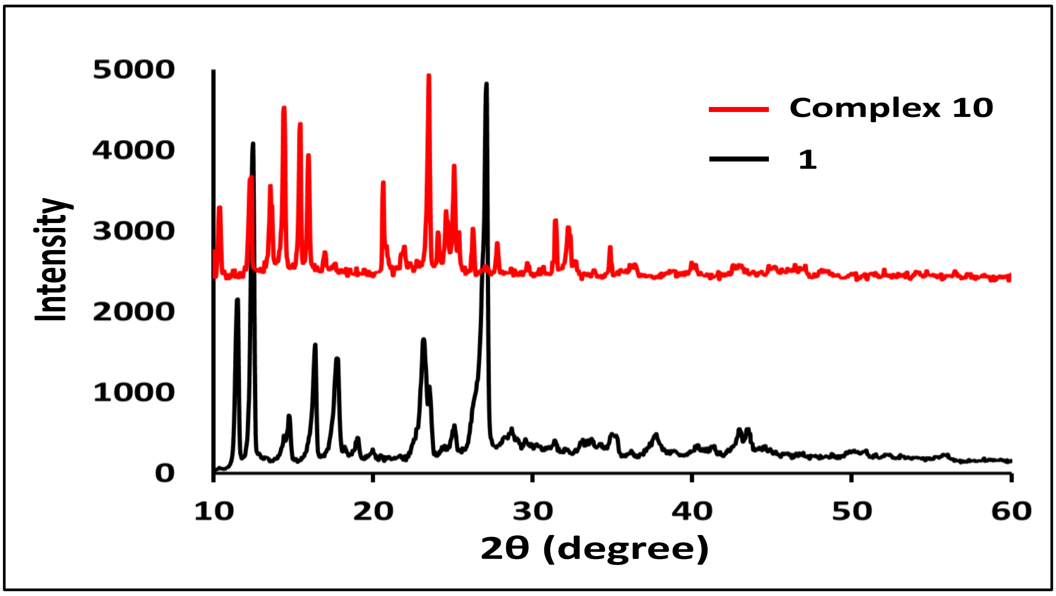

Figure 5.5 Powder XRD pattern of complex 10 overlayed with 1

The disappearance of peaks at 2θ = 11.52°, 27.11°, 37.74° and appearance of new peak at 2θ = 10.76°, 13.90°, 15.75°, 20.94°, 22.26°, 24.33°, 25.34°, 26.50°. 29.99°, 31.62°, and 32.48° confirms the formation of **complex 10.** The change in diffraction pattern are in well agreement with previously reported oxovanadium (IV) complexes [27]. The diffraction pattern also confirms the crystalline nature of **1** and **complex 10.**

5.2.3 DFT based Frontier Molecular Orbital analysis

The ground state geometry of complex 10 was fully optimized in gas phase using B3LYP/6-311G (d,p) and LanL2DZ basis sets. The optimized geometry of complex 10 found to be octahedral based on bong angle and bond length obtained from DFT calculation. Selected bond length and bond angles of **complex 10** are listed in **table S1** [28]. The negative values of frontier molecular orbitals (FMOs) indicated stability of **complex 10** [29]. The Literature reports suggested that the compounds with a small energy gap possess higher chemical reactivity, low kinetic stability, and soft in nature, vice versa for compounds that possess the high energy gap [30–32]. The global reactivity parameters along with HOMO and LUMO energy gap values are provided in **table S2**. The compositions of atomic orbitals of **complex 10** derived from FMOs along with optimized structure and MEP diagram are shown in f**igures 5.6a** and **5.6b.**

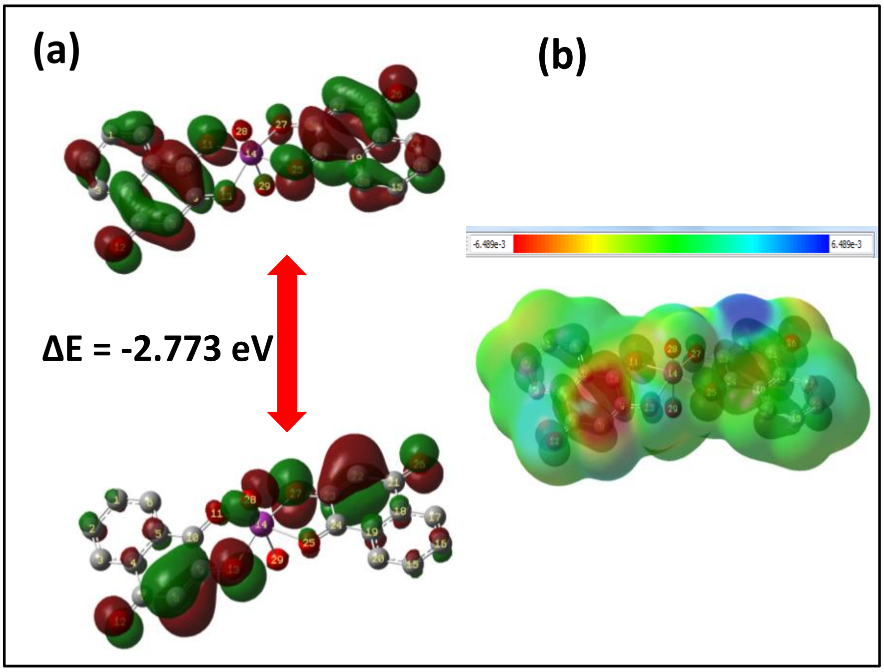

Figure 5.6 (a) Surface plot showing the frontier molecular orbitals, and (b) MEP surface diagram of complex 10

Molecular electrostatic potential (MEP) is widely used as a reactivity map. The MEP diagram can display electrophilic sites and nucleophilic sites based on electrostatic potentials [29,33]. The MEP diagram showed red region (electrophilic site) near the O atom of V=O and naphthoquinone ring, while blue region (nucleophilic site) near attached benzene ring. This result confirms the formation of **complex 10.**

5.3 Catalytic application

Synthesized **complex 10** was utilized for oxidation of diphenyl methane to benzophenone. The reaction was performed as per the conditions mentioned in **table 5.2**. Firstly, we have started with H_2O_2 as oxidant. The observed values for isolated yield was trace **(table 5.2, entry 1)**. The isolated yield increased to 51% when reaction was carried out at 50°C. However, no significant change in isolated yield was observed when reaction was stirred for 72 hr **(table 5.2, entry 2&3)**. This could be due to the fast decomposition of H_2O_2 (without being involved in the oxidation) in solvent [34]. The low yields might be due to formation of intermediate (diphenyl carbinol) over benzophenone. The formation of diphenyl carbinol intermediate and benzophenone were confirmed by ^{1}H NMR spectroscopy after purification of crude product using column chromatography.

On literature survey, we found that Tan et al. reported benzylic C_{sp3}-H bond to ketone using different oxidants at 130°C. They found TBHP to be the most suitable oxidant for transformation among screened organic peroxides for reaction [35]. Thus, changing oxidant from H_2O_2 to TBHP increased the isolated yield and conversion (conversion was monitored by GCMS) **(table 5.2, entry 4).** It was observed that, the conversion was increased (75%) when the reaction was carried out at 50°C. However, no significant increase in conversion was observed on increasing reaction time **(table 5.2, entry 5 & 6).** Surprisingly, the conversion was decreased 62% at 70°C **(table 5.2, entry 7)**. The conversion was increased to 96% when amount of TBHP increased to 1.5 mL (i.e. 11 mmol) **(table 5.2, entry 8).** Furthermore, no significant change in conversion and isolated yield was observed on increasing the amount of catalyst up to 50 mg. **(table 5.2, entries 9 & 10).** Thus we have selected **entry 8** as optimised condition for selective oxidation of diphenyl methane to benzophenone.

Table 5.2 Optimization of reaction parameters for complex 10 as catalyst

Sr. No.	Oxidant (mL)	Solvent [a]	Catalyst (mg)	Temp. (°C)	Time (h)	% yield [b]
1.	H_2O_2 (3)	Acetonitrile	30	30	72	trace
2.	H_2O_2 (3)	Acetonitrile	30	50	48	51
3.	H_2O_2 (3)	Acetonitrile	30	50	72	55
4.	TBHP (1)	Acetonitrile	30	30	72	62 (67)[c]
5.	TBHP (1)	Acetonitrile	30	50	24	70 (75) [c]
6.	TBHP (1)	Acetonitrile	30	50	36	81 (86) [c]
7.	TBHP (1)	Acetonitrile	30	70	36	58 (62) [c]
8.	**TBHP (1.5)**	**Acetonitrile**	**30**	**50**	**6**	**92 (96) [c]**
9.	TBHP (1.5)	Acetonitrile	40	50	6	92 (95) [c]
10.	TBHP (1.5)	Acetonitrile	50	50	6	90
11.	TBHP (1.5)	Methanol	30	50	6	28
12.	TBHP (1.5)	Ethanol	30	50	6	30
13.	TBHP (1.5)	Ethyl acetate	30	50	6	37
14.	TBHP (1.5)	Acetone	30	50	6	30
15.	TBHP (1.5)	DCM	30	40	6	trace
16.	TBHP (1.5)	THF	30	50	6	35
17.	TBHP (1.5)	-	30	50	36	35
18.	TBHP (1.5)	Acetonitrile	-	50	36	trace

a) Solvent (5 mL), b) Isolated yield, c) %yield by GCMS

To evaluate the solvent effect on oxidation of diphenylmethane, the reaction was carried out in different solvents under the similar reaction conditions. The solvent variations were done from polar parotic to polar aprotic and also extended to non-polar. However, there was no significant improvement in isolated yield **(table 5.2, entries 11 to 16)**. These data confirms that acetonitrile is best solvent for selective catalytic oxidation of diphenyl methane. Controlled experiments revealed that without solvent and catalyst yield were very low even after 36 h. Thus we have selected **entry 8** as optimised condition for selective oxidation of diphenyl methane to benzophenone.

Table 5.3 catalytic oxidation of aryl alkanes with complex 10 in acetonitrile[a]

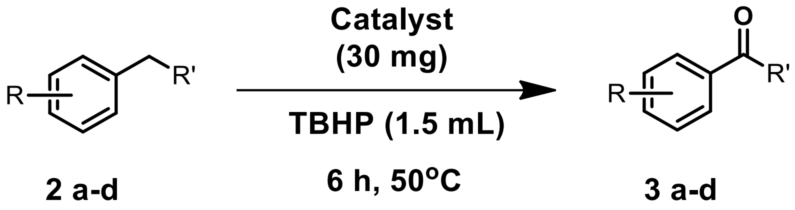

Entry	Substrate (2 a-d)	Product (3 a-d)	Yield (%)[b]
1.	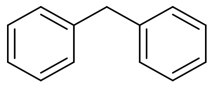	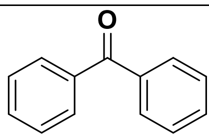	93
2.	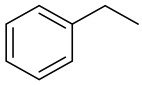	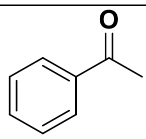	83
3.	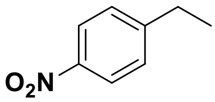	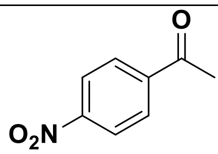	75
4.	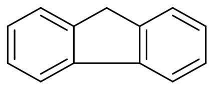	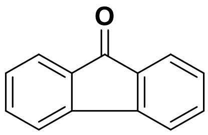	91

[a] **Reaction conditions:** substrate (1.5 mmol), catalyst (30 mg), TBHP (1.5 mL), acetonitrile (5 mL), 50°C, 6 h. [b] Isolated yield

The oxidations of several substrates were investigated in light of the aforementioned findings, and the outcomes are reported in Table 2. It was possible to oxidise every substrate that was tested to its corresponding aromatic ketones. Moderate yield of aromatic ketones was achieved when aryl alkanes with nitro substitution **(2c)** at the para position was utilised **(table 5.3, entry 3)**. We were ecstatic to discover that the substrate fluorene **(2d)** could be oxidised to fluorenone **(3d)** with a excellent yield **(table 5.3, entry 4).** According to the data above, synthesised complex **10** was an effective catalyst for oxidation reactions and could oxidise a variety of aryl alkanes to aromatic ketones with good to excellent yields when conditions were favourable.

5.4 Experimental

5.4.1 Material and methods

Vanadyl acetylacetonate purchased from Sigma-Aldrich, Mumbai, India and used as received. Lawsone was procured from TCI chemicals, Mumbai, India. 70% aqueous solution of tertiary butyl hydrogen peroxide (TBHP) was procured from avra chemicals, Mumbai, India, Hydrogen peroxide (30% W/W aqueous solution) procured from Merck, India. The reaction progress was monitored by TLC in ultraviolet light. Merck TLC plates were used to monitor the reaction progress. UV-Visible spectra were recorded on Agilent UV Cary 60 and Perkin Elmer Lambda-35 dual-beam spectrophotometer. The description of instruments used for FT-IR, NMR, elemental, and Mass analysis is depicted in **chapter 2 (section 2.3.1)**. ESR spectra was recorded using Bruker Biospin ESR spectrometer operating with X-band (9.6 GHz) microwave at 100K temperature in a suitable solvent. GCMS of samples were recorded using thermo scientific trace GC ultra with MS detector. Powder XRD was recorded on Bruker D2-Phased instrument with Lynux-eye detector.

5.4.2 Synthesis of complex 10

Vanadyl acetylacetonate (0.5 mmol) dissolved in ethanol (15 mL) was added dropwise to the suspension of **1** (1 mmol) in ethanol (20 mL). The resulting clear brownish solution was continuously stirred for 12 h at 30 ^{o}C. Then reaction mixture was concentrated under vacuum and left it overnight. The brownish crystalline product was obtained. The product was filtered and given washing with hot water followed by chilled ethanol. The obtained crystalline product was dried under vacuum. The schematic for synthesis of **complex 10** from **1** is shown in **scheme 5.1.**

Complex 10

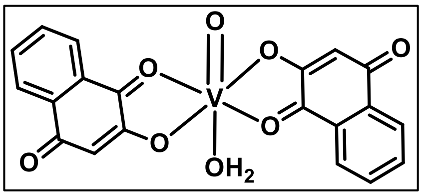

Brown crystalline powder; Yield: 69%; M.P: 180 ^{o}C

IR (KBr) cm^{-1}: 3389 (O-H), 3222 (C-H), 2924 (C-H), 1650 (C=O), 1617 (C=O), 1254 (C-O), 990 (V=O), **UV-Vis (Methanol) λ/nm, (log ε):** 430 (2.37), 690 (1.940), **ESI/MS**

431.1 $[M+1]^+$ For $C_{20}H_{12}O_8V$**, Molar conductance:** 11 S cm^2 mol^{-1}

5.4.3 Computational Studies

As described in chapter 3 and 4, Computational studies of synthesized complex **10** were carried out using Gaussian 16 software. Density functional theory (DFT) calculation was assigned to optimize the geometry of the complex using B3LYP/6-311G(d,p) and LanL2DZ basis sets. Frontier molecular orbitals and HOMO-LUMO energy gap of the complex were visualized with the aid of the Gauss View 6 visualization program.

5.4.4 Catalytic oxidation of aryl alkenes

The catalytic oxidation of aryl alkenes was carried out in a 25 ml round bottom flask. Aryl alkene (1.5 mmol) and 30 mg catalyst (complex 10, 0.06 mmol) were stirred in 5 mL acetonitrile. Then 1.5 mL aqueous tert-butyl hydrogen peroxide (70% TBHP, 11.1 mmol) was added and stirred the reaction mixture at 50°C for 6 h. The progress of the reaction was monitored by TLC. After completion of the reaction, the solvent was evaporated under vacuum and extracted in hexane (product extracted in hexane was given for GC-MS analysis to determine selectivity and conversion for optimised conditions only). Hexane was evaporated and the product was purified by column chromatography to obtain white crystalline solid. The Schematic for oxidation is shown in **scheme 5.2.**

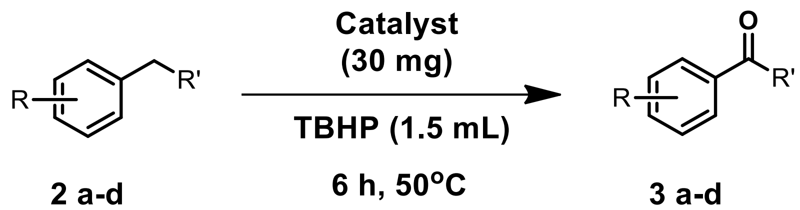

Scheme 5.2 Schematic for catalytic oxidation of aryl alkenes

Benzophenone (3a)

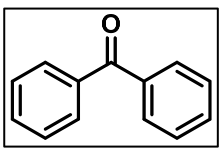

White solid; Yield: 93%; M.P: 50 °C

^{1}H NMR ($CDCL_3$, 400 MHz) δ (ppm): 7.47 (t, *J*=1.6 Hz, *J*=7.7 Hz, 2H), 7.58 (tt, *J*=2.5 Hz, *J*=3.4 Hz, *J*= *7.4* Hz 1H), 7.79 (dd, *J*=1.45 Hz, *J*=4.7 Hz, 2H) **(figure S5.1)**

Acetophenone (3b)

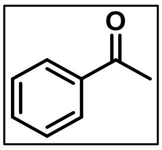

Colourless liquid; Yield: 83%

^{1}H NMR ($CDCL_3$, 400 MHz) δ (ppm): 7.96-7.94 (m, 2H), 7.57-7.53 (m, 1H), 7.47-7.43 (m, 2H), 2.59 (s, 3H) **(figure S5.2)**

1-(4-nitrophenyl)ethanone (3c)

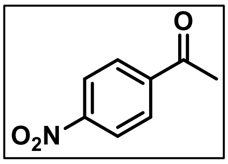

Light yellow crystals; Yield: 75%; M.P: 76 ^{o}C

^{1}H NMR ($CDCL_3$, 400 MHz) δ (ppm): 8.32-8.29 (m, 2H), 8.13-8.10 (m, 2H), 2.69 (s, 3H) **(figure S5.3)**

9H-fluoren-9-one (Fluorenone) (3d)

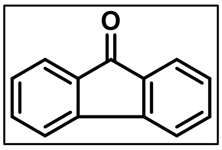

Light yellow crystals; Yield: 91%; M.P: 81 ^{o}C

^{1}H NMR ($CDCL_3$, 400 MHz) δ (ppm): 7.69-7.55 (m, 1H), 7.54-7.50 (m, 2H), 7.33-7.28 (m, 1H) **(figure S5.3)**

5.5 Conclusion

In summary, a vanadium (IV) complex was created from naturally occurring lawsone and characterised using a variety of spectroscopic methods, including powder XRD, FTIR, UV, and mass spectrometry. Additionally, DFT computations verified the complex's creation and established the optimised geometry. Furthermore, it was used for the high conversion and 92% isolated yield of diphenylmethane with TBHP at 50°C in acetonitrile. Additionally, it preferentially transforms substituted arylalkanes into the appropriate ketones. This study can be studied for various substituted arylalkanes and in organic synthesis, and it may offer some guidelines for future use.

5.6 Spectra and Figures

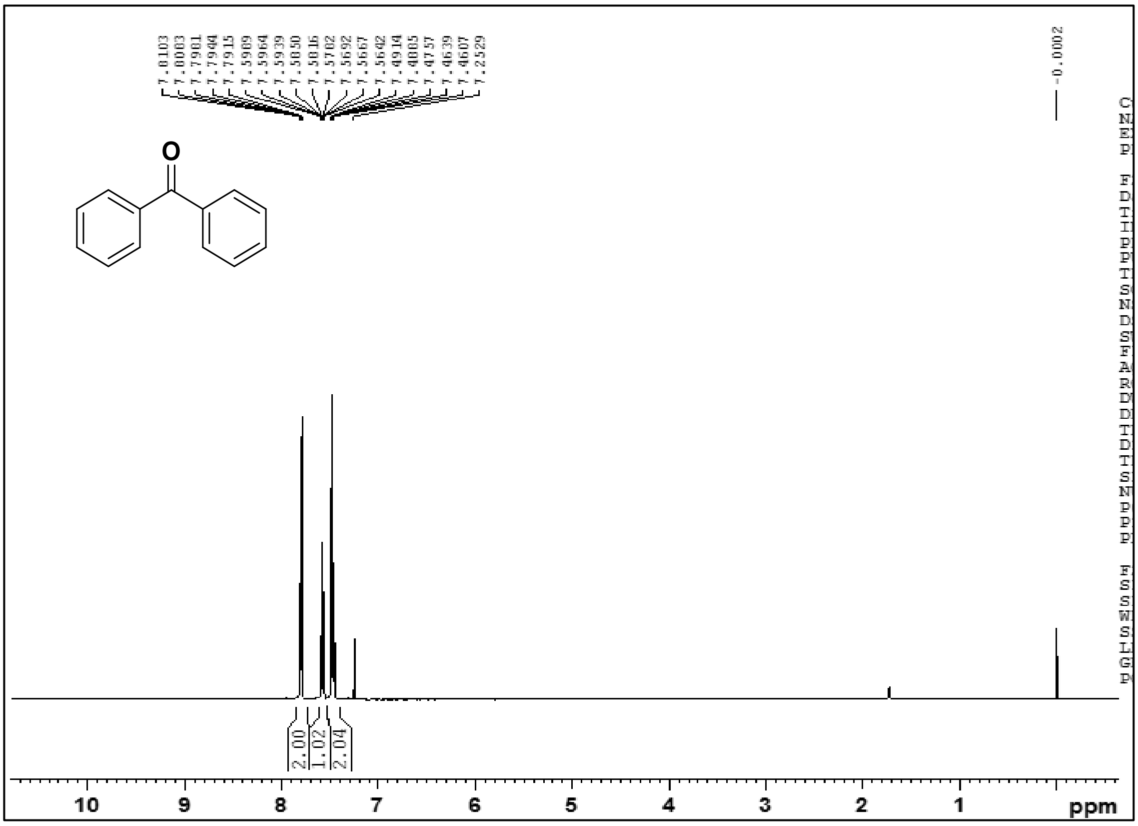

Figure S5.1 ^{1}H NMR spectra of benzophenone (3a)

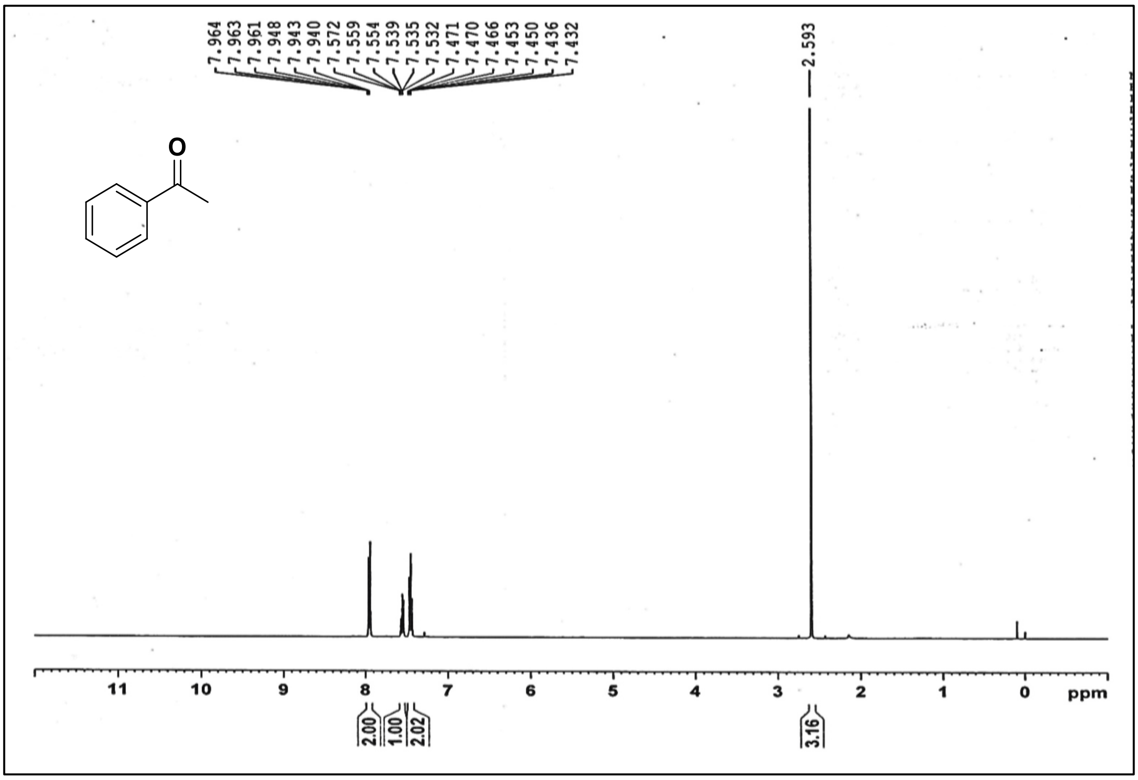

Figure S5.2 ^{1}H NMR spectra of acetophenone (3b)

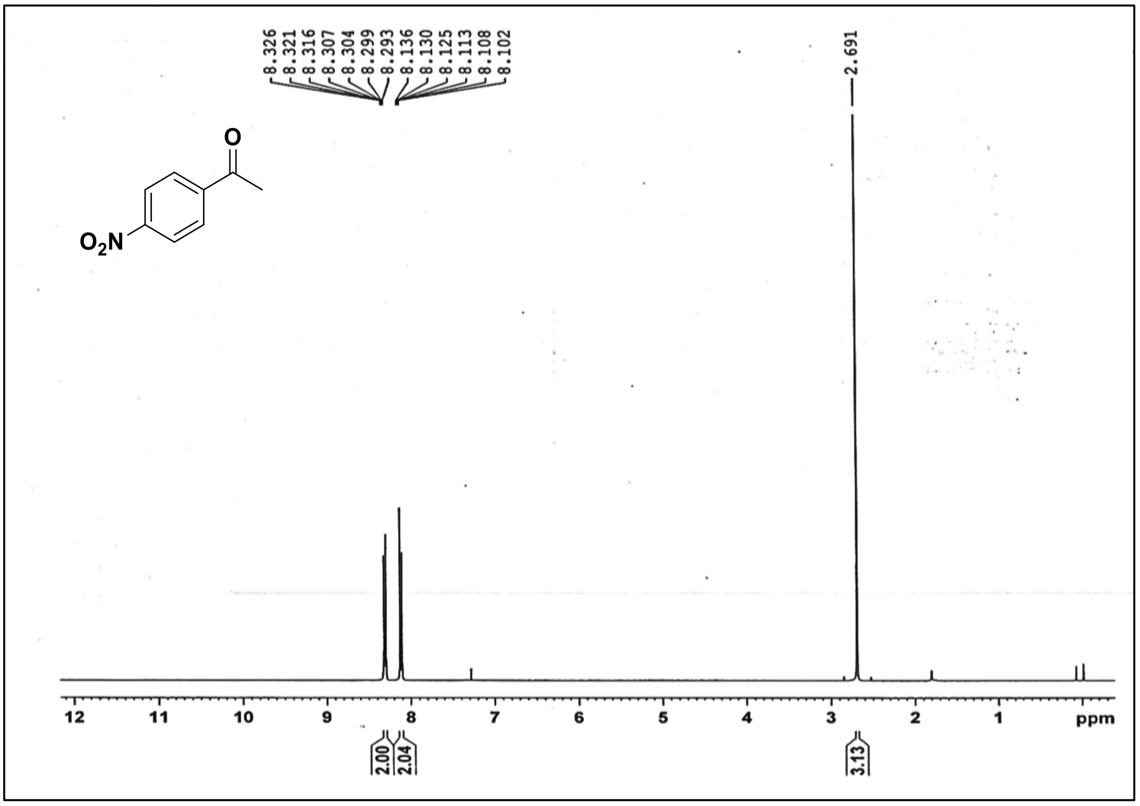

Figure S5.3 ^{1}H NMR spectra of 1-(4-nitrophenyl)ethanone (3c)

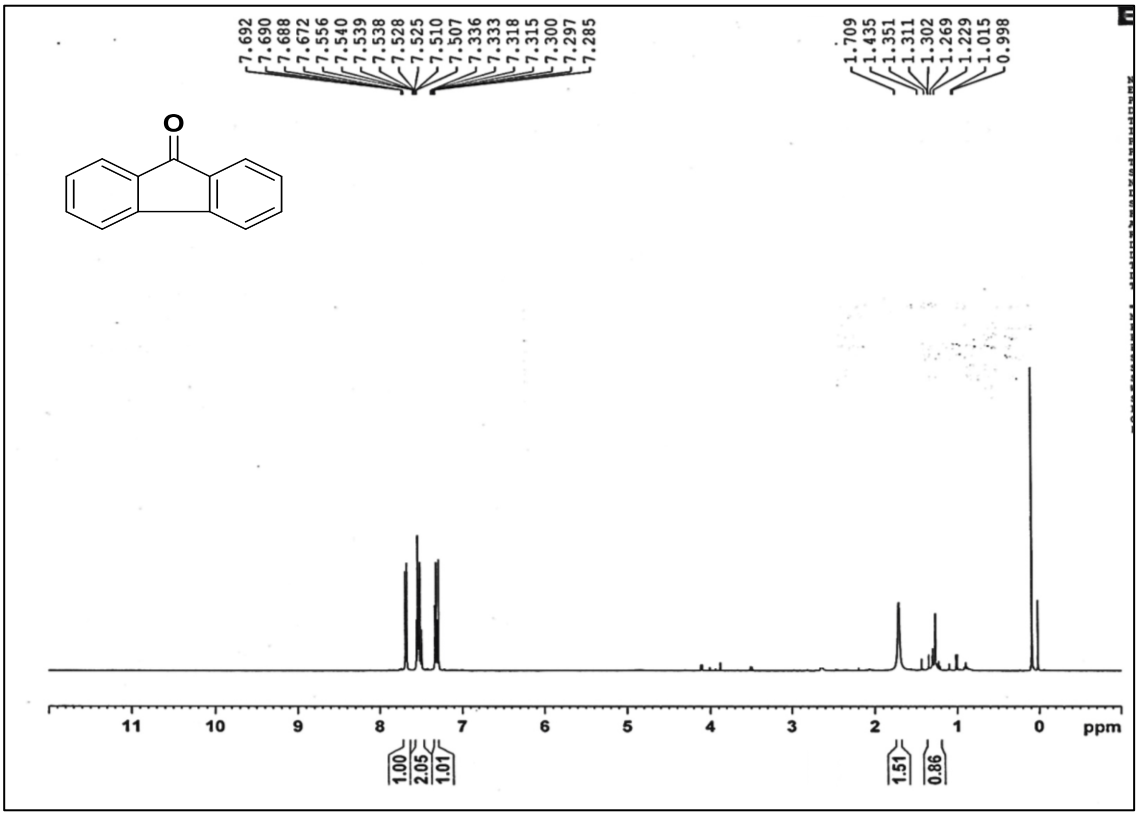

Figure S5.4 ^{1}H NMR spectra of 9H-fluoren-9-one (Fluorenone) (3d)

5.7 References

1. Newhouse, T. & Baran, P. S. If C À H Bonds Could Talk : Selective C À H Bond Oxidation. 3362–3374 (2011) doi:10.1002/anie.201006368.

2. Shang, C. & Liu, Z. Origin and Activity of Gold Nanoparticles as Aerobic Oxidation Catalysts in Aqueous Solution. 9938–9947 (2011).

3. Karimov, R. R. & Hartwig, J. F. Mild metal-catalyzed C–H activation: examples and concepts. 2900–2936 (2016) doi:10.1039/C6CS00075D.

4. Gensch, T., Hopkinson, M. N. & Glorius, F. Chem Soc Rev Mild metal-catalyzed C – H activation : examples. *Chem. Soc. Rev.* 2900–2936 (2016) doi:10.1039/c6cs00075d.

5. Shaabani, A., Farhangi, E. & Rahmati, A. Aerobic oxidation of alkyl arenes and alcohols using cobalt(II) phthalocyanine as a catalyst in 1-butyl-3-methyl-imidazolium bromide. *Appl. Catal. A Gen.* **338**, 14–19 (2008).

6. bin Saiman, M. I. *et al.* Involvement of Surface-Bound Radicals in the Oxidation of Toluene Using Supported Au-Pd Nanoparticles. *Angew. Chemie* **124**, 6083–6087 (2012).

7. Zhou, H. *et al.* Defect-less, layered organo-titanosilicate with superhydrophobicity and its catalytic activity in room-temperature olefin epoxidation. *Chem. Commun.* **48**, 6954–6956 (2012).

8. Surana, K., Chaudhary, B., Diwaker, M. & Sharma, S. Benzophenone: a ubiquitous scaffold in medicinal chemistry. *Medchemcomm* **9**, 1803–1817 (2018).

9. Zhou, M. *et al.* Cp * Iridium Precatalysts for Selective C − H Oxidation with Sodium Periodate As the Terminal Oxidant. (2013).

10. Wang, Y., Kuang, Y. & Wang, Y. Rh2(esp)2-catalyzed allylic and benzylic oxidations. *Chem. Commun.* **51**, 5852–5855 (2015).

11. Smith, M. W. *et al.* Applied Catalysis A : General Carbon formation on Rh-substituted pyrochlore catalysts during partial oxidation of liquid hydrocarbons. *"Applied Catal. A, Gen.* **502**, 96–104 (2015).

12. Sharma, A. S. & Kaur, H. Sustainable Protocol for Benzylic -CH 2 Oxidation with Dioxygen to Phenones Using AuNPs @ Resin Beads. 10112–10117 (2017) doi:10.1002/slct.201702157.

13. Complexes, R. V. Oxidation and Amination of Benzylic sp 3 C − H Bond Catalyzed by Rhenium(V) Complexes. **3**, (2012).

14. Xia, J. B., Cormier, K. W. & Chen, C. A highly selective vanadium catalyst for benzylic C-H oxidation. *Chem. Sci.* **3**, 2240–2245 (2012).

15. Shen, D., Miao, C., Wang, S., Xia, C. & Sun, W. E ffi cient Benzylic and Aliphatic C − H Oxidation with Selectivity for Methylenic Sites Catalyzed by a Bioinspired Manganese Complex. (2013).

16. Luo, J., Yu, H., Wang, H. & Peng, F. Enhancing the catalytic activity of carbon nanotubes by fi lled iron nanowires for selective oxidation of ethylbenzene. *CATCOM* **51**, 77–81 (2014).

17. Chan, S. I. *et al.* Efficient Oxidation of Methane to Methanol by Dioxygen Mediated by Tricopper Clusters ** Angewandte. 1–6 (2013) doi:10.1002/anie.201209846.

18. Damian P. Hruszkewycz, a Kelsey C. Miles, a O. R. T. and S. S. S. Co/NHPI-mediated aerobic oxygenation of benzylic C–H bonds in pharmaceutically relevant molecules. *Chem. Sci.* 1282–1287 (2017) doi:10.1039/c6sc03831j.

19. Hong Yi, A., Changliang Bian, A., Xia Hu, A., Linbin Niu, A. & Lei, and A. ChemComm. (2015) doi:10.1039/C5CC06015J.

20. Alanthadka, A. *et al.* NHC-Catalyzed Benzylic C sp^3 -H Bond Activation of Alkylarenes and N -Benzylamines for the Synthesis of 3 H -Quinazolin-4-ones: Experimental and Theoretical Study. *European J. Org. Chem.* **2016**, 4872–4880 (2016).

21. Ma, J. *et al.* DDQ / tert -Butyl nitrite-catalyzed aerobic oxidation of diarylmethane sp 3 C e H bonds. *Tetrahedron* **71**, 6733–6739 (2015).

22. Yin, L., Wu, J., Xiao, J. & Cao, S. Oxidation of benzylic methylenes to ketones with Oxone – KBr in aqueous acetonitrile under transition metal free conditions. *Tetrahedron Lett.* **53**, 4418–4421 (2012).

23. Borah, R., Lahkar, S., Deori, N. & Brahma, S. Synthesis, characterization and application of oxovanadium(<scp>iv</scp>) complexes with [NNO] donor ligands: X-ray structures of their corresponding dioxovanadium(<scp>v</scp>) complexes. *RSC Adv.* **12**, 13740–13748 (2022).

24. Sanasam, B., Raza, M. K., Musib, D. & Roy, M. Photochemical and photocytotoxic evaluation of new Oxovanadium (IV) complexes in photodynamic application. *J. Chem. Sci.* **133**, (2021).

25. Han, H. *et al.* Synthesis and evaluation of oxovanadium(iv) complexes of Schiff-base condensates from 5-substituted-2-hydroxybenzaldehyde and 2-substituted-benzenamine as selective inhibitors of protein tyrosine phosphatase 1B. *Dalt. Trans.* **41**, 11116 (2012).

26. Yuan, C. *et al.* Synthesis, characterization, and protein tyrosine phosphatases inhibition activities of oxovanadium(IV) complexes with Schiff base and polypyridyl derivatives. *J. Inorg. Biochem.* **104**, 978–986 (2010).

27. Chang, Y. P., Furness, L., Levason, W., Reid, G. & Zhang, W. Complexes of vanadium(IV) oxide difluoride with neutral N- and O-donor ligands. *J. Fluor. Chem.* **191**, 149–160 (2016).

28. Biswal, D. *et al.* Synthesis, crystal structure, DFT calculations, protein interaction, anticancer potential and bromoperoxidase mimicking activity of oxidoalkoxidovanadium(V) complexes†. *New J. Chem.* **43**, 17783–17800 (2019).

29. Khan, I. M. *et al.* Exploring interaction dynamics of designed organic cocrystal charge transfer complex of 2-hydroxypyridine and oxalic acid with human serum albumin: Single crystal, spectrophotometric, theoretical and antimicrobial studies. *Bioorg. Chem.* **100**, 103872 (2020).

30. Murugavel, S., Ravikumar, C., Jaabil, G. & Alagusundaram, P. Synthesis, crystal structure analysis, spectral investigations (NMR, FT-IR, UV), DFT calculations, ADMET studies, molecular docking and anticancer activity of 2-(1-benzyl-5-methyl-1H-1,2,3-triazol-4-yl)-4-(2-chlorophenyl)-6-methoxypyridine – A novel poten. *J. Mol. Struct.* **1176**, 729–742 (2019).

31. Krishnan, K. G. *et al.* Novel cyanoacetamide integrated phenothiazines: Synthesis, characterization, computational studies and in vitro antioxidant and anticancer evaluations. *J. Mol. Struct.* **1199**, 127037 (2020).

32. Khan, I. M. & Shakya, S. Exploring Colorimetric Real-Time Sensing Behavior of a Newly Designed CT Complex toward Nitrobenzene and Co2+: Spectrophotometric, DFT/TD-DFT, and Mechanistic Insights. *ACS Omega* **4**, 9983–9995 (2019).

33. Rocha, M. *et al.* Diethylaminophenyl-based Schiff base Cu(ii) and V(iv) complexes: Experimental and theoretical studies and cytotoxicity assays. *New J. Chem.* **43**, 18832–18842 (2019).

34. Kishore, D. & Rodrigues, A. E. Liquid phase selective oxidation of diphenylmethane to benzophenone over ternary hydrotalcites with tert-butylhydroperoxide. *Catal. Commun.* **10**, 1212–1215 (2009).

35. Tan, J., Zheng, T., Yu, Y. & Xu, K. TBHP-promoted direct oxidation reaction of. 15176–15180 (2017) doi:10.1039/c7ra00352h.